



Identification of IQM-266, a Novel DREAM Ligand That Modulates K_v4 Currents

Diego A. Peraza^{1,2†}, Pilar Cercós^{3†}, Pablo Miaja¹, Yaiza G. Merinero¹, Laura Lagartera³, Paula G. Socuélamos^{1,4}, Carolina Izquierdo García³, Sara A. Sánchez¹, Alejandro López-Hurtado^{5,6}, Mercedes Martín-Martínez³, Luis A. Olivos-Oré⁴, José R. Naranjo^{5,6}, Antonio R. Artalejo⁴, Marta Gutiérrez-Rodríguez^{3*} and Carmen Valenzuela^{1,2*}

¹Instituto de Investigaciones Biomédicas Alberto Sols (IIBM), CSIC-UAM, Madrid, Spain, ²Spanish Network for Biomedical Research in Cardiovascular Research (CIBERCv), Instituto de Salud Carlos III, Madrid, Spain, ³Instituto de Química Médica (IQM), IQM-CSIC, Madrid, Spain, ⁴Instituto Universitario de Investigación en Neuroquímica & Departamento de Farmacología y Toxicología, Facultad de Veterinaria, UCM, Madrid, Spain, ⁵Centro Nacional de Biotecnología (CNB), CNB-CSIC, Madrid, Spain, ⁶Spanish Network for Biomedical Research in Neurodegenerative Diseases (CIBERNED), Instituto de Salud Carlos III, Madrid, Spain

OPEN ACCESS

Edited by:

Lane Brown,
Washington State University,
United States

Reviewed by:

Ying Zhang,
Dalhousie University, Canada
Thomas Budde,
University of Münster, Germany

*Correspondence:

Marta Gutiérrez-Rodríguez
mgutierrez@iqm.csic.es
Carmen Valenzuela
cvalenzuela@iib.uam.es

[†]These authors have contributed
equally to this work

Received: 03 October 2018

Accepted: 14 January 2019

Published: 04 February 2019

Citation:

Peraza DA, Cercos P, Miaja P, Merinero YG, Lagartera L, Socuélamos PG, Izquierdo García C, Sánchez SA, López-Hurtado A, Martín-Martínez M, Olivos-Oré LA, Naranjo JR, Artalejo AR, Gutiérrez-Rodríguez M and Valenzuela C (2019) Identification of IQM-266, a Novel DREAM Ligand That Modulates K_v4 Currents. *Front. Mol. Neurosci.* 12:11. doi: 10.3389/fnmol.2019.00011

Downstream Regulatory Element Antagonist Modulator (DREAM)/KChIP3/calsenilin is a neuronal calcium sensor (NCS) with multiple functions, including the regulation of A-type outward potassium currents (I_A). This effect is mediated by the interaction between DREAM and K_v4 potassium channels and it has been shown that small molecules that bind to DREAM modify channel function. A-type outward potassium current (I_A) is responsible of the fast repolarization of neuron action potentials and frequency of firing. Using surface plasmon resonance (SPR) assays and electrophysiological recordings of $K_v4.3$ /DREAM channels, we have identified IQM-266 as a DREAM ligand. IQM-266 inhibited the $K_v4.3$ /DREAM current in a concentration-, voltage-, and time-dependent-manner. By decreasing the peak current and slowing the inactivation kinetics, IQM-266 led to an increase in the transmembrane charge ($Q_{K_v4.3/DREAM}$) at a certain range of concentrations. The slowing of the recovery process and the increase of the inactivation from the closed-state inactivation degree are consistent with a preferential binding of IQM-266 to a pre-activated closed state of $K_v4.3$ /DREAM channels. Finally, in rat dorsal root ganglion neurons, IQM-266 inhibited the peak amplitude and slowed the inactivation of I_A . Overall, the results presented here identify IQM-266 as a new chemical tool that might allow a better understanding of DREAM physiological role as well as modulation of neuronal I_A in pathological processes.

Keywords: $K_v4.3$ channels, DREAM, DREAM ligands, KChIP, A-type current, Alzheimer

INTRODUCTION

The Downstream Regulatory Element Antagonist Modulator (DREAM; Carrion et al., 1999), also known as KChIP3 (An et al., 2000) or calsenilin (Buxbaum et al., 1998), is a member of the K_v channel interacting proteins (KChIPs) belonging to the neuronal calcium sensor (NCS) family (Burgoyne, 2007). DREAM is a 29 kDa protein with four EF-hand motif (EF1–4), conserved among other NCS members, in which the EF2 mediates low affinity Ca^{2+} binding and is occupied by Mg^{2+}

under physiological conditions, whereas EF3 and EF4 mediate high affinity Ca²⁺ binding (Bahring, 2018). The physiological roles of DREAM have been gradually revealed. In the nucleus, DREAM binds to a specific DRE to repress transcription of target genes (Carrion et al., 1999; Cheng et al., 2002; Ruiz-Gomez et al., 2007; Wu et al., 2010). Outside the nucleus, DREAM interacts with presenilins to modulate calcium release from the endoplasmic reticulum (Lilliehook et al., 2002). Additionally, the role of the downregulation of DREAM as part of an endogenous neuroprotective mechanism that improves ATF6 processing, neuronal survival in the striatum, and motor coordination in R6/2 mice, a model of Huntington's disease (HD), has been recently described (Naranjo et al., 2016; López-Hurtado et al., 2018). Besides, DREAM acts as a regulatory subunit of K_V4.3 channels by inducing: (i) increased traffic of K_V4.3 channels to the membrane; (ii) delayed inactivation kinetics; and (iii) accelerated activation and recovery kinetics from inactivation of K_V4.3 channels (An et al., 2000). K_V4 α -subunits, KChIPs and dipeptidyl aminopeptidase-like proteins (DPPs) form ternary complexes, which regulate the A-type outward potassium currents in neurons (*I_A*; Nadal et al., 2003; Maffie and Rudy, 2008). *I_A* is responsible for the fast repolarization of neuron action potentials and the frequency of firing, and thereby controls neuronal excitability (Birnbaum et al., 2004; Johnston et al., 2010). Among the K_V4 α -subunits, K_V4.2 and K_V4.3 underlie the somatodendritic *I_A* in the central nervous system (CNS; Huang et al., 2005), whereas, K_V4.1 mRNA levels are lower than K_V4.2 or K_V4.3 (Seródio and Rudy, 1998). Among other KChIPs, DREAM binding to K_V4 channels regulates potassium currents, and hence neuronal excitability, in response to changes in intracellular calcium. Alterations in the function of the complexes K_V4/KChIP and/or DREAM are implicated in different neuronal pathologies such as Alzheimer's (Hall et al., 2015) and HD (Naranjo et al., 2016), spinocerebellar ataxia (Smets et al., 2015) or epilepsy (Villa and Combi, 2016). Additionally, small molecules that bind to DREAM also modify channel function (Gonzalez et al., 2014; Naranjo et al., 2016). In this regard, repaglinide and CL-888 showed an inhibition of the *I_A* (Naranjo et al., 2016), whereas NS5806 is the only described DREAM ligand showing a potentiation of *I_A* under certain conditions (Witzel et al., 2012). Hence, it would be of great interest to have broader range of chemical tools that might allow a better understanding of the physiological role of DREAM and the modulation of neuron *I_A* in pathological processes.

In this work, using surface plasmon resonance (SPR) assays and electrophysiological recordings of K_V4.3/DREAM channels, we described IQM-266 as a new DREAM ligand able to inhibit the K_V4.3/DREAM current in a concentration- and voltage-dependent manner, and to slow the activation and the inactivation kinetics. Blocking the peak current and slowing the inactivation kinetics led to an increase in the transmembrane charge ($Q_{K_{V4.3}/DREAM}$) at a certain range of concentrations, identifying IQM-266 as a new activator of the DREAM-mediated K_V4.3 currents. Importantly, *I_A* recording from rat dorsal root ganglia (DRG) neurons revealed IQM-266 effects reminiscent

of those observed in K_V4.3/DREAM channels. Our findings offer new possibilities to control neuronal hyperexcitability by modulating the potassium outward current through K_V4 channel complexes.

MATERIALS AND METHODS

All experiments shown in the present study were performed through the NIH rules (Guide for the care and use of laboratory animals; NIH publications number 23-80) revised in 2011; as well as the European Parliament 2010/63/EU and the rules of the Helsinki Declaration.

IQM-266 Chemical Synthesis

3-(2-(3-Phenoxyphenyl)acetamido)-2-naphthoic acid: 2-(3-phenoxyphenyl)acetic acid (1.5 equiv.) in SOCl₂ (2 mL/mmol) was refluxed for 6 h, and the excess of thionyl chloride was evaporated to dryness. The residue was then dissolved in anhydrous THF (2 mL/mmol), and 3-amino-2-naphthoic acid (1.0 equiv.) and propylene oxide (15.0 equiv.) were added to the solution. After stirring overnight at room temperature, the solvent was evaporated to dryness and the crude residue was dissolved in EtOAc (3 × 10 mL), washed with brine (30 mL) and dried over Na₂SO₄. After removal of the solvent to dryness, the residue was triturated with Et₂O, and the resultant solid subsequently triturated with CH₃CN. The obtained solid was lyophilized to give a brown pale solid. m.p. 198.1–196.3°C. ¹H-NMR (400 MHz, dimethyl sulfoxide (DMSO)-*d*₆) δ (ppm): 3.81 (s, 2H, CH₂CO), 6.94 (ddd, *J* = 8.2, 2.5, 0.9 Hz, 1H, H_{4'}), 7.03 (dt, *J* = 7.7, 1.1 Hz, 2H, H_{2'',6''}), 7.07 (t, *J* = 2.5 Hz, 1H, H_{2'}), 7.11 (tt, *J* = 7.7, 1.1 Hz, 1H, H_{4''}), 7.17 (dt, *J* = 8.2, 0.9 Hz, 1H, H_{6'}), 7.33–7.41 (m, 3H, H_{5',3'',5''}), 7.47 (ddd, *J* = 8.1, 6.9, 1.1 Hz, 1H, H₆), 7.60 (ddd, *J* = 8.1, 6.9, 1.1 Hz, 1H, H₅), 7.86 (d, *J* = 8.1 Hz, 1H, H₇), 8.01 (d, *J* = 8.1 Hz, 1H, H₄), 8.67 (s, 1H, H₈), 8.94 (s, 1H, H₃), 11.12 (s, 1H, NH). ¹³C-NMR (100 MHz, DMSO-*d*₆) δ (ppm): 44.3 (CH₂CO), 116.6 (C₃), 117.3 (C₁), 117.4 (C_{4'}), 118.5 (C_{2'',6''}), 120.0 (C_{2'}), 123.4 (C_{4''}), 124.9, 125.6 (C_{6'}), 127.1, 128.2, 129.1, 129.3, 130.0 (C_{3'',5''}), 130.2 (C_{5'}), 133.1 (C_{7a}), 135.5 (C_{3a}), 136.0 (C₂), 137.0 (C_{1'}), 156.7 (C_{3',1''}), 168.6 (CO₂H), 169.4 (CH₂CO). HPLC (Sunfire C18, gradient 50%–95% of acetonitrile in water, 10 min): t_R = 7.04 min. LC-MS: 398.2 ([M + H]⁺). HRMS (EI⁺) *m/z* found 397.1306 ([M]⁺ C₂₅H₁₉NO₄ calculated 397.1314).

Surface Plasmon Resonance (SPR): Binding Experiments

SPR experiments were performed at room temperature (20°C) with a Biacore X-100 apparatus (Biacore, GE Healthcare Life Sciences) in running buffer (50 mM Tris pH 7.5, 50 mM NaCl, 2 mM CaCl₂ with 2% DMSO and 0.05% Tween 20). The protein GST-DREAM was immobilized on a CM5 sensor chip (Biacore, GE) following a standard amine coupling method (Johnsson et al., 1991). The carboxymethyl dextran surface of the experimental flow cell was activated with a 7-min injection of a 1:1 ratio of 0.4 M 1-ethyl-3-(3-dimethylaminopropyl)carbodiimide hydrochloride (EDC) and 0.1 M *N*-hydroxysuccinimide. The protein was coupled

to the surface with a 7-min injection at several dilutions at 10–100 $\mu\text{g/ml}$ in 10 mM sodium acetate, pH 4.0. Unreacted *N*-hydroxysuccinimide esters were quenched by a 7-min injection of 0.1 M ethanolamine-HCl (pH 8.0). Immobilization levels were in the 7,000–8,000 RUs range. Reference flow cell was treated as experimental flow cell (amine coupling procedure) but without protein. Prior to use, 10 mM stock solutions of IQM-266 compound were diluted several times to a 1–7 μM final concentration in running buffer. Affinity measurements were made by a series of different concentrations injected onto the sensor chip at a 90 $\mu\text{l/min}$ flow rate for 1 min, followed by a 1 min dissociation period. After dissociation, an extra wash was done over the flow cells with 50% DMSO. No regeneration was needed.

Sensograms data were double-referenced and solvent-corrected using the BIAevaluation X-100 software (Biacore, GE Healthcare Life Sciences). Experimental data for affinity measurements were adjusted to a one site-specific model binding with Hill slope, using the equation: $R_{\text{eq}} = R_{\text{max}}[A]^n / (K_D^n + [A]^n)$ where R_{eq} is the equilibrium response at each concentration, R_{max} is the maximum specific binding, $[A]$ is the analyte concentration, K_D the equilibrium dissociation constant and n the Hill slope.

Cellular Cultures and Transient Transfection

All experiments were performed in CHO-K1 (*Chinese Hamster Ovary*, CHO) cells obtained from the American Type Culture Collection (Rockville, MD, USA) and cultured at 37°C in Iscove's modified Eagle's medium supplemented with 10% (v/v) fetal bovine serum (FBS), 1% (v/v) L-Glutamine (Gibco), and antibiotics (100 IU/ml penicillin and 100 mg/ml streptomycin; all from Gibco, Paisley, UK) in a 5% CO₂ atmosphere.

Cells were transiently cotransfected with Kv4.3 (cloned into pEGFPn1, gently given by Dr. D.J. Synders, University of Antwerpen, Belgium) and DREAM (cloned into pcDNA3.1). In both cases, cells were cotransfected with EBO-pcDLeu2 as a reporter gene, codifying CD8. Transfection was performed using Fugene-6 (Promega) following manufacturer's instructions as previously described (Moreno et al., 2017; López-Hurtado et al., 2018). After 48 h transfection, cells were removed from culture plates using TrypLE™ Express (Life Technologies), after exposing them to polystyrene microspheres bound to anti-CD8 (Dynabeads M-450, Thermo Fisher Scientific; Franqueza et al., 1999; Naranjo et al., 2016). Because the level of expression of DREAM can be crucial for the effects of IQM-266, only cells cotransfected with Kv4.3 and DREAM that exhibit a recovery kinetics from inactivation between 20 and 45 ms were selected for electrophysiological recording.

Electrophysiology

Potassium currents elicited by the activation of Kv4.3/DREAM channels expressed in CHO cells were recorded at room temperature (20–25°C), at a frequency of 0.1 Hz using the whole-cell patch-clamp technique with an Axopatch 200B patch-clamp amplifier (Molecular Devices) connected to an analogic

digital converter (Digidata 1322A). Micropipettes were pulled from borosilicate glass capillary tubes (Narishige GD-1) on a programmable horizontal puller (Sutter Instrument Co.) and heat-polished with a microforge (Narishige, Japan). Micropipette resistance was 2–4 M Ω . Data acquisition and genesis of experimental protocols were performed by the CLAMPX utility of the PCLAMP 9.0.1 program (Molecular Devices). Currents were filtered at 2 kHz and sampled at 4 kHz (Bessel filter of 4 poles). Capacitance and series resistance compensation were optimized, with 80% compensation of the effective access resistance usually obtained. The intracellular pipette filling solution contained (in mM): 80 K-aspartate, 42 KCl, 3 phosphocreatine, 10 KH₂PO₄, 3 MgATP, 5 HEPES-K, 5 EGTA-K and it was adjusted to pH 7.25 with KOH. The bath solution contained (in mM): 136 NaCl, 4 KCl, 1.8 CaCl₂, 1 MgCl₂, 10 HEPES-Na and 10 glucose and it was adjusted to pH 7.40 with NaOH. IQM-266 was dissolved in DMSO at a stock concentration of 5 mM and added to the external solution at the desired concentration in each experiment. The currents were stored in a computer and analyzed with the CLAMPFIT utility of the PCLAMP 9.0.1 program and Origin 2018 (OriginLab Co.). Origin 2018 (OriginLab Co.) and Clampfit 10 programs were used to perform least-squares fitting and for data presentation (Valenzuela et al., 1994; Longobardo et al., 1998; Naranjo et al., 2016).

In order to obtain the concentration-response curve, block produced by IQM-266 was measured at the maximum peak and under the area of the current after applying different concentrations of the compound (0.01–100 μM) and thus, $\%block = \left(1 - \left(\frac{I_{\text{Drug}}}{I_{\text{Control}}}\right)\right) \times 100$. From the fitting of these values to a Hill equation, concentration-effect curves were generated, obtaining the values of the IC₅₀ and the Hill coefficient (n).

Activation and inactivation were fitted to a monoexponential process with an equation of the form $y = Ae^{(-\frac{t}{\tau})} + C$, where τ represents the system time constant, A represents the amplitude of the exponential, and C is the baseline value. The voltage dependence of the activation curves was fitted with a Boltzmann equation: $y = 1 / \left(1 + e^{-(V-V_h)/s}\right)$, where s represents the slope factor, V represents the membrane potential, and V_h represents the voltage at which 50% of the channels are open. Recovery from inactivation was analyzed by applying a two pulse protocol consisting in a prepulse from –80 to +60 mV of 1 s in duration, followed by a test pulse to +60 mV of 250 ms in duration after different recovery time. The current measured at the maximum peak and the current in the test pulse were normalized vs. the first prepulse and they were plotted against the recovery time and then fitted to a monoexponential equation in order to obtain the τ_{re} (view “Results” section). In all cases, the control and the experimental condition was the same cell before and after being exposed to IQM-266.

Isolation of DRG Neurons and Recording of Transient Potassium Currents (I_A)

DRG neurons were isolated from male Sprague-Dawley rats (200–220 g/6–8 weeks old). Rats were sacrificed by cervical

dislocation followed by decapitation, and lumbar segments of the spinal column were removed and placed in a cold Ca²⁺, Mg²⁺-free Hank's solution (Sigma-Aldrich). The bone surrounding the spinal cord was removed and L4, L5 and L6 DRG were exposed and pulled out. After removing the roots, DRG were chopped in half and incubated for 60 min at 37°C in Dulbecco's modified Eagle's Medium-low glucose (DMEM; Sigma-Aldrich) containing 5 mg/mL collagenase XI (Worthington Biochemical, Lakewood, NJ, USA), 100 U/ml penicillin (Sigma-Aldrich), and 0.1 mg/ml streptomycin (Sigma-Aldrich). The cell suspension was then washed with DMEM by centrifugation (300 g, 5 min at 4°C), filtered through a 100 μm mesh and washed again by centrifugation. The cell pellet was resuspended in DMEM and 40 μl were dropped onto 10 mm diameter glass coverslips treated with poly-D-lysine (1 mg/ml, 30 min; Sigma-Aldrich) and placed in 35 mm diameter Petri dishes. Finally, plated cells were flooded with 2.5 ml of DMEM and supplemented with 10% fetal calf serum (BioWhittaker, UK), 100 U/ml penicillin and 0.1 mg/ml streptomycin, stored in an incubator (Hera Cell, Heraeus, Germany) at 37°C under a 5% CO₂/95% air atmosphere. This protocol yields spherical cell bodies without neurites, from which only medium DRG neurons (30–40 μm diameter; 30–50 pF) were chosen for recording within 12–24 h of plating.

Current recordings were performed at room temperature (21–24°C) in the perforated-patch variant of the whole-cell configuration of the patch-clamp technique, with an EPC10 amplifier using PatchMaster software (HEKA Electronic, Lambrecht, Germany; Carabelli et al., 2003). Patch pipettes were pulled from borosilicate glass to have a final resistance of 5.5–6.5 MΩ when filled with internal solution (see below). Membrane currents were filtered at 3 kHz and sampled at 10 kHz from cells held at a voltage of –80 mV. Series resistance (<20 MΩ) was compensated by 80% and monitored together with the cell membrane capacitance throughout the experiment. The perforated-patch configuration was obtained using amphotericin B (Sigma-Aldrich) dissolved in DMSO and stored at –20°C in aliquots of 50 mg/ml. The pipette-filling solution contained (mM) 90 K₂SO₄, 55 KCl, 8 NaCl, 1 MgCl₂, 15 HEPES (pH 7.2 with KOH; ≈280 mOsm). Fresh pipette solution was prepared every 2 h. The bath solution containing (mM) 145 NaCl, 2.8 KCl, 2 CaCl₂, 1 MgCl₂, 10 HEPES, and 10 glucose (pH 7.4 adjusted with NaOH; ≈300 mOsm) was constantly superfused at a rate of approximately 1 ml/min. IQM-266, at the desired concentration (3 or 10 μM), was directly applied onto the cell under investigation by gravity from a multibarrel concentration-clamp device coupled to electronically driven miniature solenoid valves. The common outlet of this was placed within 100 μm of the cell to be patched.

Transient potassium current (*I_A*) was isolated by using voltage protocols, taking advantage of the distinct voltage-dependent inactivation of the underlying potassium channels (Phuket and Covarrubias, 2009). First, total voltage-activated potassium current was measured in cells held at –80 mV, in which a 1-s conditioning pulse to –100 mV was delivered prior to 250-ms step depolarizations, ranging from –20 to +20 mV in 10 mV increments. Then, a depolarizing 1-s conditioning pulse

to –20 mV was applied, sufficient to inactivate *I_A*, such that the outward current evoked by subsequent step depolarizations was mostly comprised of a delayed rectifying potassium current. *I_A* was finally revealed by subtracting the delayed rectifying current from total current. Peak amplitude of *I_A* was used to determine percent block by IQM-266. *I_A* inactivation was fitted to a biexponential process with an equation of the form:

$$y = y_0 + A_f \exp\left(\frac{-(x - x_0)}{\tau_f}\right) + A_s \exp\left(\frac{-(x - x_0)}{\tau_s}\right)$$

where τ_f and τ_s represent the fast and slow time constants, respectively, and A_f and A_s represent the amplitudes of the corresponding kinetic components.

Statistics

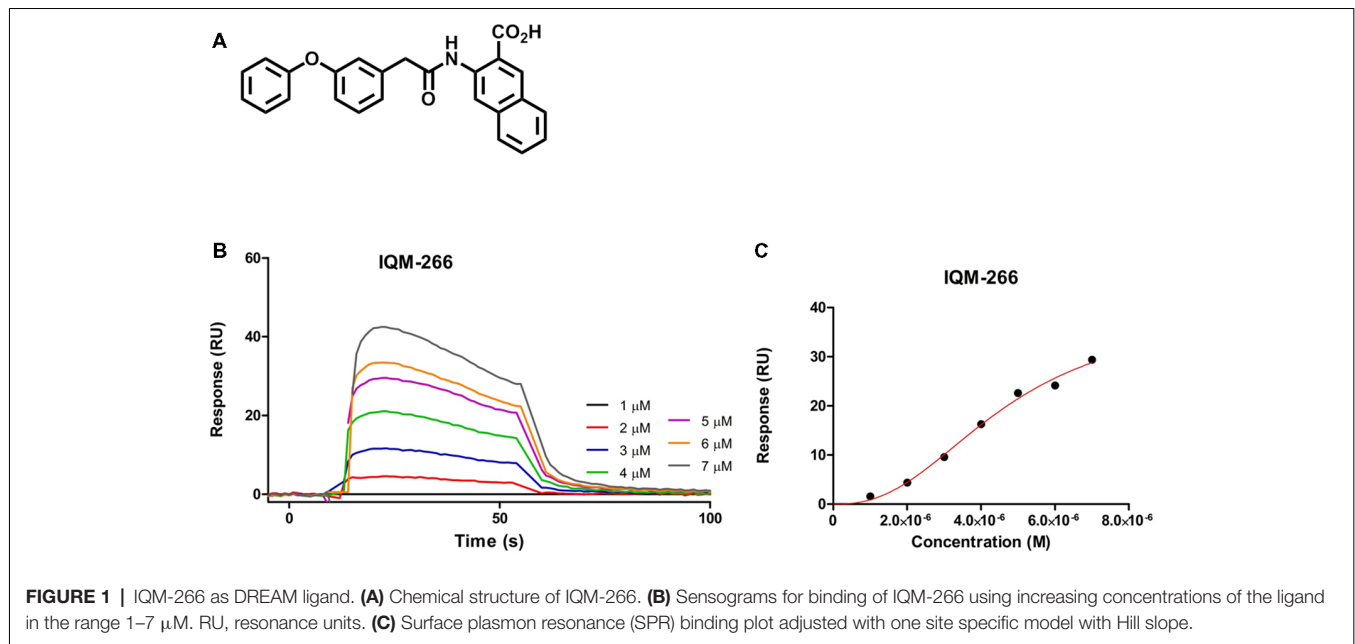
Data are expressed as the mean ± SEM. Direct comparisons between mean values in control conditions and in the presence of drug for a single variable were performed by paired Student's *t*-test. Differences were considered significant if the *p* value was less than 0.05.

RESULTS

Identification of IQM-266 as DREAM Ligand Modulator of K_V4.3/DREAM Channel Activity

As part of our program of medicinal chemistry searching for DREAM ligands, we performed a high throughput screening of our chemical libraries to evaluate their binding to DREAM using SPR. We selected the novel compound 3-(2-(3-Phenoxyphenyl)acetamido)-2-naphthoic acid, IQM-266, which showed a $K_D = 4.63 \pm 0.73 \mu\text{M}$, and we have investigated its effect on the K_V4/DREAM channels currents (**Figure 1**; for synthesis and full characterization of IQM-266 see “Materials and Methods” section).

Figure 2A shows the concentration-dependence of block produced by IQM-266 on K_V4.3/DREAM channels when measured at the maximum peak current. By fitting these data to a Hill equation, the concentration that inhibited 50% of the channels (IC_{50}) and the Hill coefficient (*n*) were calculated (8.6 μM and 0.75, respectively, *n* = 34). **Figure 2A** also shows the Hill fit in which we assume that this curve exhibits a basal value of 0 and a maximum percentage block of 100 (dashed line). The IC_{50} and the *n* obtained with this fit were very similar to those obtained without any constriction (9.0 μM and 1.0, respectively). The *n* value obtained led us to conclude that binding of IQM-266 to K_V4.3/DREAM channels does not exhibit cooperativity. **Figure 2B** exhibits a bar graph in which the effects of this compound on the maximum peak current and on the charge (measured as the integral of the current recordings) are shown. At all concentrations tested, IQM-266 decreased the maximum peak current and, to a lesser extent, the charge through the membrane, these differences being very marked between 1 and 10 μM. Indeed, at 3 μM, IQM-266 decreased the maximum peak current ($33.7 \pm 5.3\%$, *n* = 6), but increased the charge ($13.0 \pm 4.1\%$, *n* = 6), which can be explained by the slowing



effect on the inactivation kinetics produced by this compound (**Figure 2C**). IQM-266 slows down both the activation and the inactivation kinetics of the current in a concentration-dependent manner. Therefore, the equilibrium between the decrease in the maximum peak current and the slowing of the inactivation process lead, either to an increase (at 3 μ M) or to a decrease in the charge (concentrations >3 μ M; **Figure 2D**). In order to characterize both effects: the increase and the inhibition of the charge through $K_V4.3$ /DREAM channels, two different concentrations of IQM-266 were used, 3 and 10 μ M (close to the IC_{50}), respectively.

Time Dependent Effects of IQM-266 on $K_V4.3$ /DREAM Channels

The activation kinetics of $K_V4.3$ /DREAM current in the absence and in the presence of IQM-266 was analyzed by fitting the traces to a monoexponential equation, from which the activation time constant (τ_{Act}) was obtained. The inactivation process was also fitted to a monoexponential curve after applying a 250 ms depolarizing pulse from -80 mV to $+60$ mV, from which the time constant of inactivation (τ_{Inac}) of the $K_V4.3$ /DREAM, in the absence and in the presence of IQM-266, were obtained (**Figure 3**). **Figures 3A,B** show the first 25 ms of the normalized currents after applying a depolarizing pulse from -100 to $+60$ mV in the absence and in the presence of 3 or 10 μ M IQM-266. In order to analyze the concentration-dependence of this slowing in the activation kinetics, the $\tau_{Ac,IQM-266}/\tau_{Ac,Control}$ ratio vs. IQM-266 concentration was plotted (**Figure 3C**). As it can be observed, the slowing effect induced by this compound was concentration-dependent. **Figure 3D** shows the absolute values under control and in the presence of IQM-266 at 3 and 10 μ M, respectively. This slowing effect on the activation kinetics was observed at membrane potentials positive to 0 mV ($p < 0.05$). This compound also slows the inactivation process at membrane

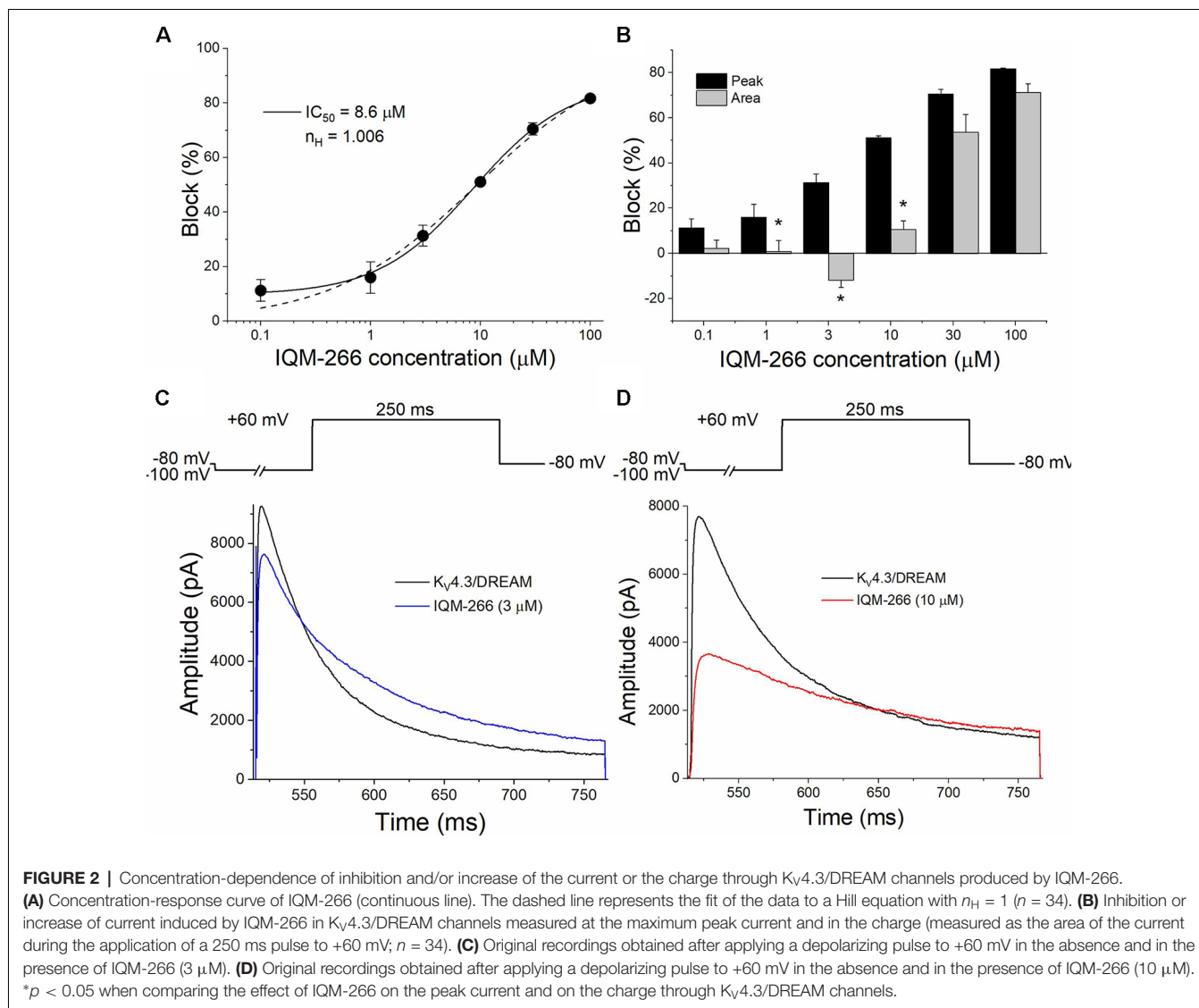
potentials positive to 0 mV ($p < 0.05$), therefore, this slowing is concentration-dependent (**Figures 3F–J**).

Effects of IQM-266 on the Recovery Kinetics of Inactivation of $K_V4.3$ /DREAM Channels

In order to analyze the recovery from inactivation of $K_V4.3$ /DREAM channels, a double pulse protocol was applied (**Figures 4A,B**, upper panel), consisting in a conditioning prepulse from -80 to $+60$ mV of 1 s in duration (I_0) in order to inactivate most of the channels, followed by a test pulse applied after a variable interpulse (between 10 and 800 ms at -90 mV) to $+60$ mV (I_t). This pulse protocol was applied before and after perfusing the cells with 3 μ M or 10 μ M IQM-266. The ratio I_t/I_0 measured at the maximum peak was plotted vs. the time interpulse between the end of I_0 and the application of I_t . In all experimental conditions, data were fitted to a monoexponential function, from which the time constant of recovery (τ_{re}) was obtained. Under control conditions, the τ_{re} arose a mean value of 42.7 ± 4.5 ms ($n = 8$). IQM-266 slowed the recovery process of the $K_V4.3$ /DREAM current in a concentration-dependent manner (from 46.8 ± 5.3 to 109.2 ± 13.0 ms in control and in the presence of IQM-266 3 μ M, $n = 5$, $p < 0.01$ and from 37.7 ± 6.9 to 153.6 ± 26.3 ms in control and in the presence of IQM-266 10 μ M $n = 4$ $p < 0.05$; **Figures 4C,D**). Interestingly, both concentrations of IQM-266 induced an overshoot in the recovery process similar to that observed in cardiac I_{to} , and that has been attributed to KCNE2 effects (Wettwer et al., 1993; Zhang et al., 2001; Radicke et al., 2008).

Voltage Dependence Effects of IQM-266 on $K_V4.3$ /DREAM Channels

Figure 5A shows superimposed current traces obtained in the absence and in the presence of IQM-266 at 3 or 10 μ M. After



plotting the maximum peak current obtained under control and after perfusion with external solution containing 3 μ M or 10 μ M IQM-266, the current-voltage (I-V) relationships were obtained (Figure 5B). These two plots also show the ratio $I_{IQM-266}/I_{Control}$ at both concentrations (blue triangles), together with the activation curve (dashed line). A block of the maximum peak current produced by IQM-266 3 μ M increased in the range of activation of $K_V4.3$ /DREAM channels but remained constant at membrane potentials positive to +10 mV. At higher concentrations, the maximum block was obtained at +20 mV ($63.1 \pm 3.6\%$, $n = 4$) and it decreased only when the more positive potential was applied ($58.8 \pm 3.0\%$ at +60 mV, $n = 4$, $p < 0.05$). Figure 5C shows the charge-voltage relationships (Q-V) obtained after plotting the charge under the current obtained in control and in the presence of IQM-266 3 or 10 μ M. These plots also show the relative charge (blue triangles) at each membrane potential in order to analyze the voltage dependence of block. IQM-266 at 3 μ M increased the charge in

a voltage independent manner. The maximum block (measured at the charge) produced by IQM-266 at 10 μ M was observed at -20 mV and this block decreased in a voltage dependent manner ($45.8 \pm 6.7\%$ vs. $23.5 \pm 4.5\%$ at -20 mV and +60 mV, respectively, $n = 4$, $p < 0.05$). Importantly; both the increase of the charge and the decrease in the maximum peak current were observed at all membrane potentials.

The activation curves were obtained from the I-V relationships. Data were plotted against membrane potential to which each current record was generated and fitted to a Boltzmann equation, in order to obtain the V_h and s values. IQM-266, at 3 μ M, did not shift the activation curve ($V_h = +4.3 \pm 2.6$ mV and $+7.8 \pm 3.9$ mV in the absence and in the presence of IQM-266, $n = 5$, $p > 0.05$; $s = 16.1 \pm 0.3$ mV and 19.6 ± 0.6 mV, $n = 5$, $p > 0.05$).

In order to study the voltage dependence of inactivation of $K_V4.3$ /DREAM channels, a double pulse protocol consisting in a 250 ms conditioning pulse to different potentials between

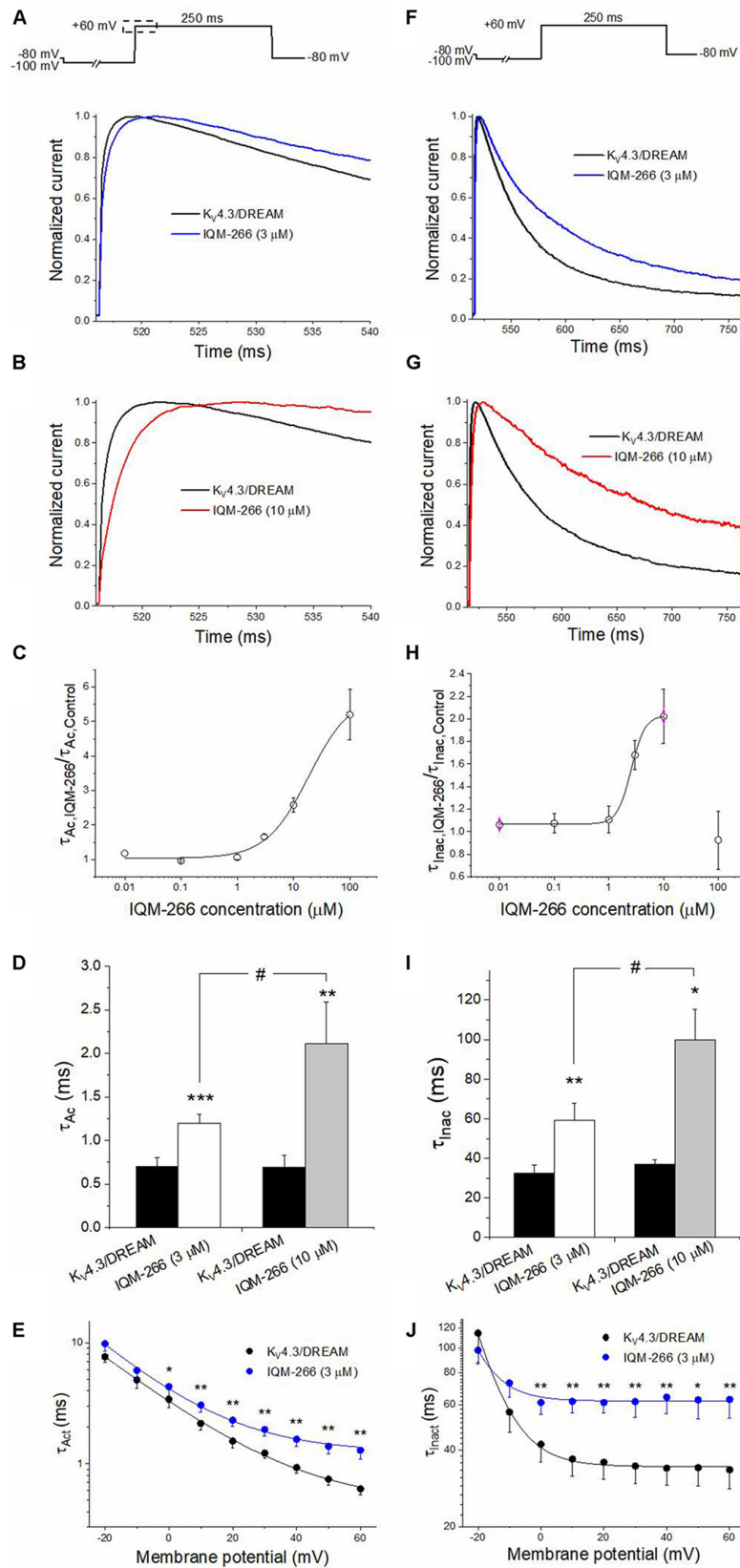


FIGURE 3 | Continued

FIGURE 3 | Activation and inactivation kinetics of $K_V4.3$ /DREAM currents in the absence and in the presence of IQM-266. **(A)** Normalized first 20 ms of original current recordings in control and in the presence of IQM-266 (3 μ M). The current records were fitted to a monoexponential equation in order to obtain the activation time constant (τ_{Ac}). **(B)** Normalized first 20 ms of original current recordings in control and in the presence of IQM-266 (10 μ M). The current records were fitted to a monoexponential equation in order to obtain the τ_{Ac} values. **(C)** Concentration-dependence of the $\tau_{Ac,IQM-266}/\tau_{Ac,Control}$. **(D)** Histogram representing the τ_{Ac} in the different experimental conditions. **(E)** Voltage-dependent effects of IQM-266 (3 μ M) on the time constant of activation (τ_{Ac}). **(F)** Normalized first 250 ms of original current recordings in control and in the presence of IQM-266 (3 μ M). The current records were fitted to a monoexponential equation in order to obtain the inactivation time constant (τ_{Inac}). **(G)** Normalized first 250 ms of original current recordings in control and in the presence of IQM-266 (10 μ M). The current records were fitted to a monoexponential equation in order to obtain the τ_{Inac} values. **(H)** Concentration-dependence of the $\tau_{Inac,IQM-266}/\tau_{Inac,Control}$. **(I)** Histogram representing the τ_{Inac} in the different experimental conditions. **(J)** Voltage-dependent effects of IQM-266 (3 μ M) on the time constant of inactivation (τ_{Inac}). * $p < 0.05$, ** $p < 0.01$ and *** $p < 0.001$ when comparing data in presence of IQM-266 with control; # $p < 0.05$ when comparing data obtained in the presence of IQM-266 (3 μ M) and IQM-266 (10 μ M).

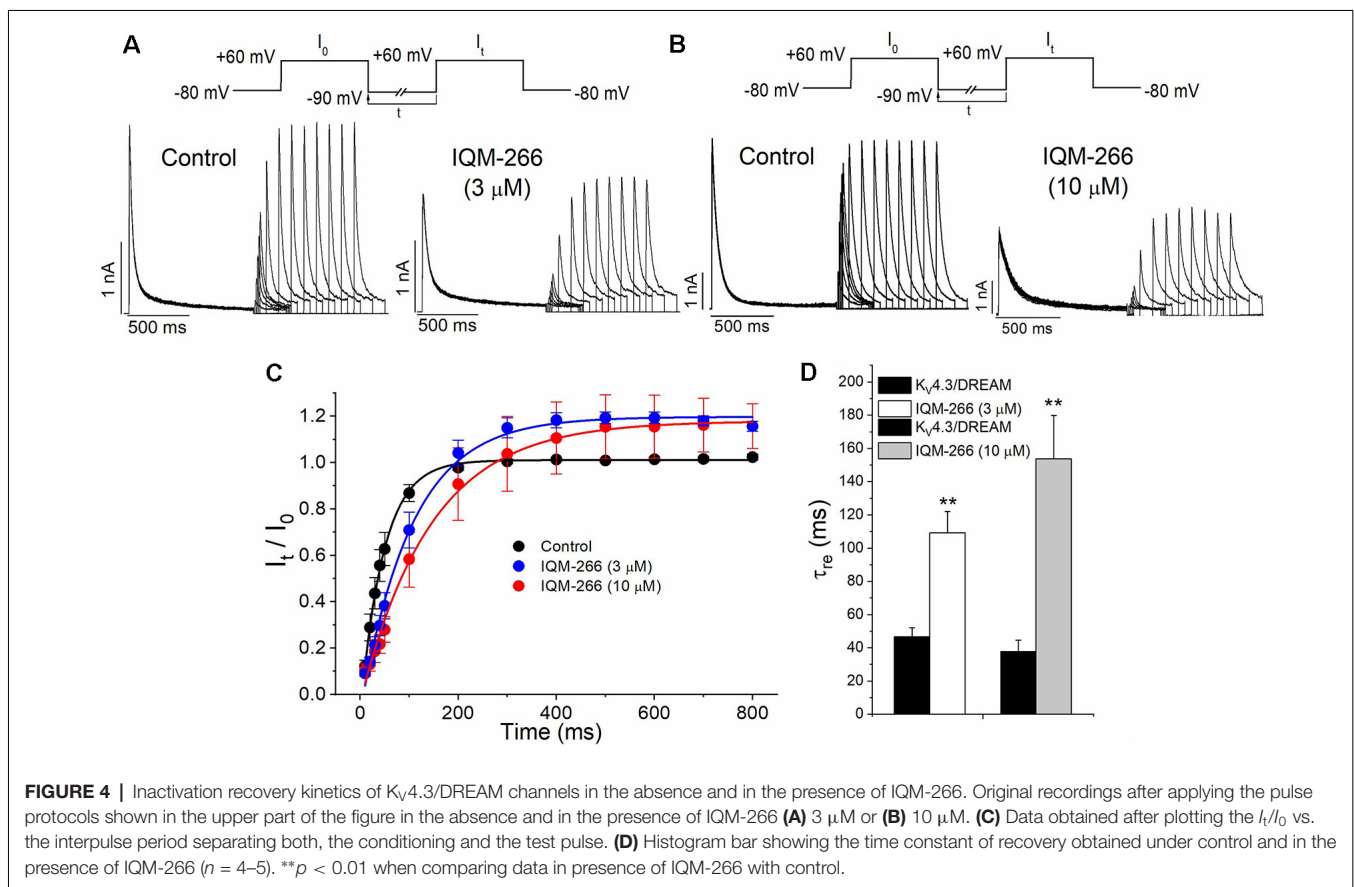
–110 and +60 mV, followed by a test pulse to +50 mV of 250 ms in duration, was applied (**Figure 6A**). The maximum peak currents measured at the test pulse were plotted against the membrane potential of the previous conditioning pulse, and the data were fitted to a Boltzmann equation. IQM-266,

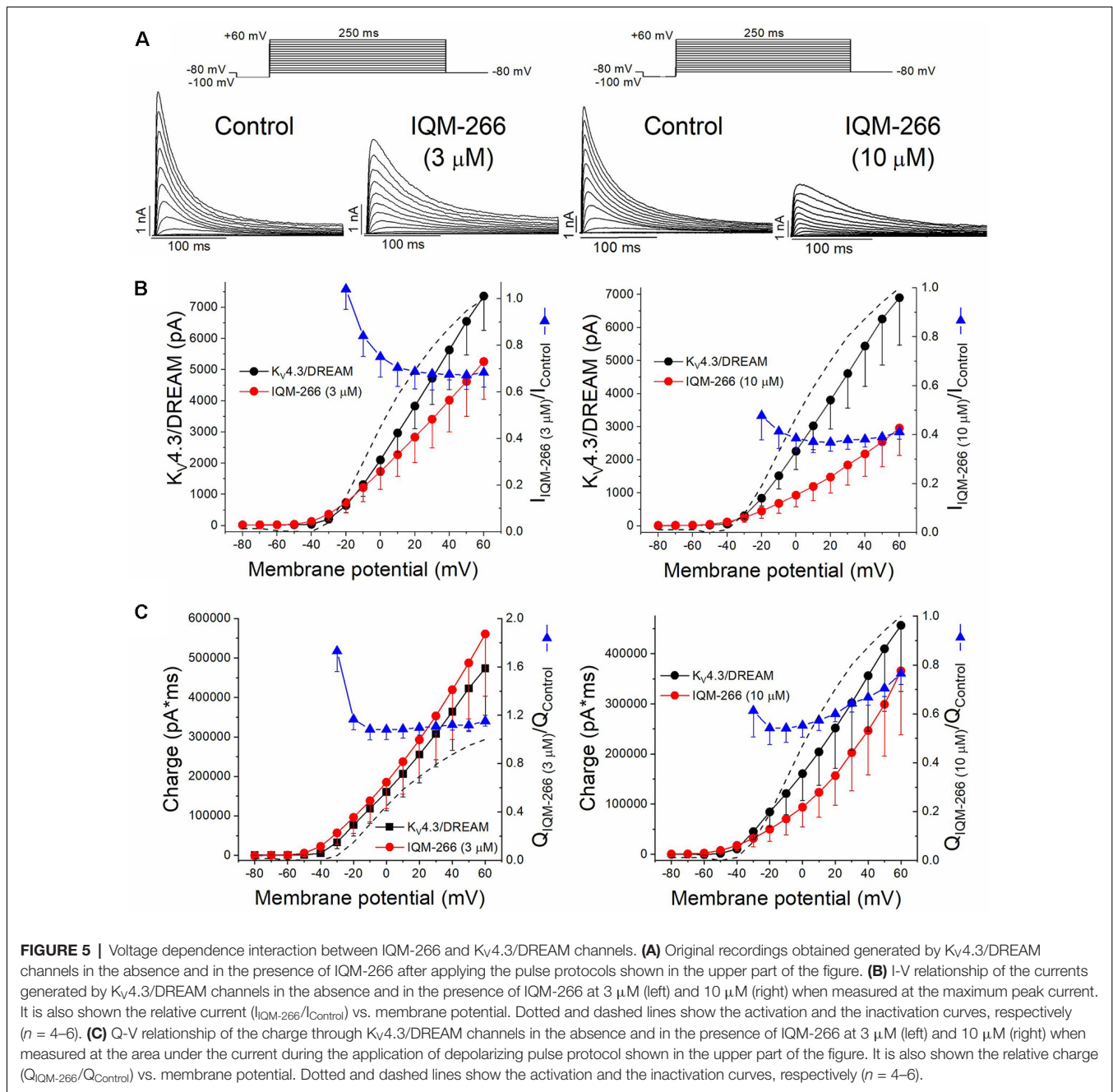
at 3 μ M, shifted the inactivation curve to negative potentials ($V_h = -30.1 \pm 0.7$ mV and -38.0 ± 0.9 mV in the absence and in the presence of IQM-266, $n = 4$, $p < 0.01$; $s = 4.5 \pm 0.2$ mV and 6.6 ± 0.7 mV, $n = 4$, $p > 0.05$; **Figure 6C**).

Since $K_V4.3$ channels inactivate predominantly from the closed state (Campbell et al., 1993; Beck and Covarrubias, 2001), the negative shift induced by IQM-266 of the steady-state inactivation curve is indicative of an acceleration of the closed-state inactivation. In order to elucidate this issue, a double pulse protocol was applied. A pre-pulse test to +60 mV during 100 ms was immediately preceded by a pulse to –40 mV of variable duration (**Figure 6B**). As it can be observed, IQM-266 increased the degree of closed-state inactivated channels, thus suggesting that IQM-266 promotes inactivation from the closed-state (**Figure 6D**).

Effects of IQM-266 on $K_V4.3$ Channels

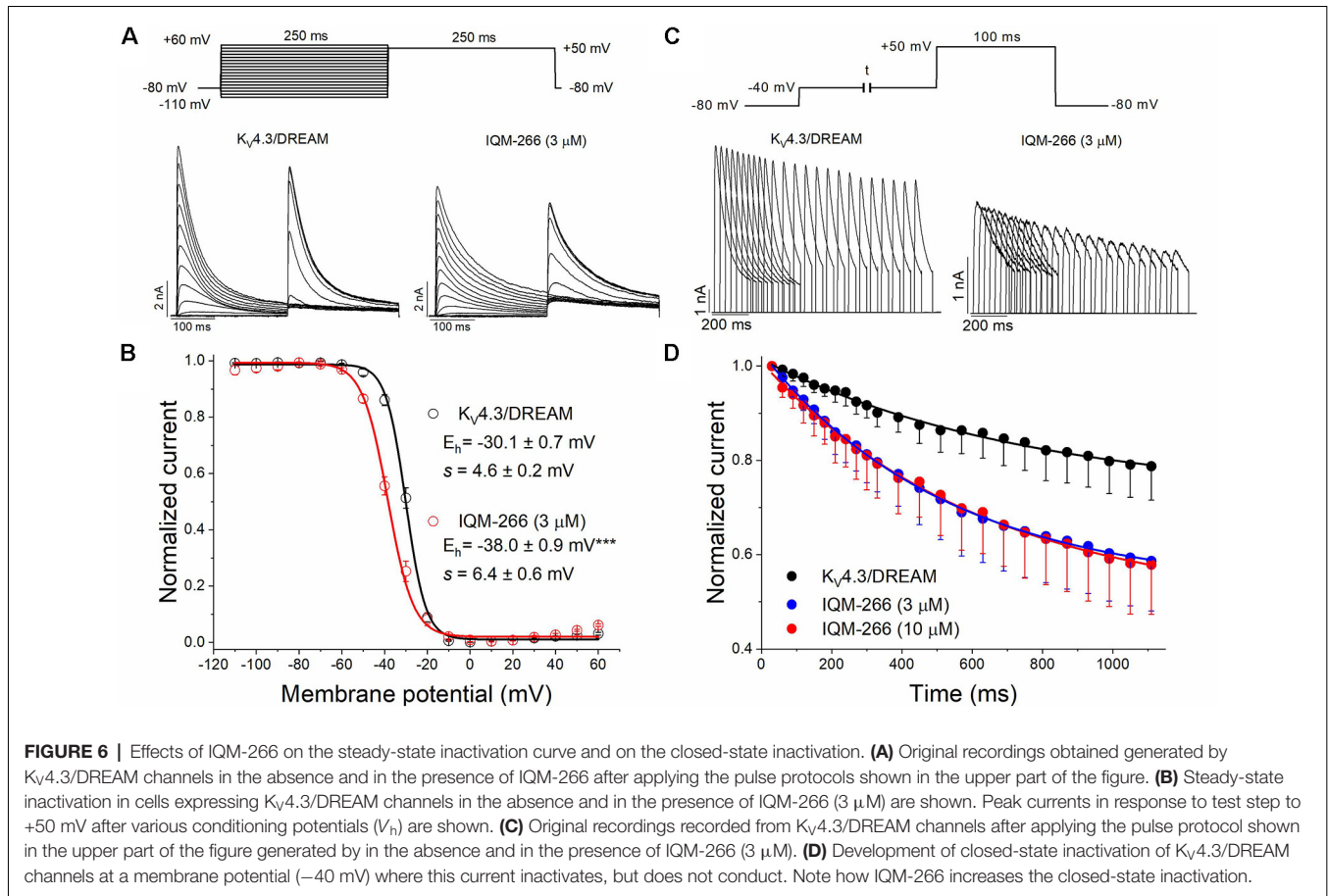
In order to analyze the selectivity of IQM-266 for $K_V4.3$ /DREAM over $K_V4.3$ channels, the effects of IQM-266 were studied on $K_V4.3$ channels expressed in CHO cells in the absence of DREAM. As it is shown in the **Figure 7**, the IC_{50} value obtained when measured at the maximum peak current was very close to that observed in $K_V4.3$ /DREAM channels (7.1 μ M vs. 8.6 μ M, $n = 21$ –23). Also, IQM-266 slowed the activation kinetics ($\tau = 0.73 \pm 0.09$ ms vs. 1.92 ± 0.32 ms, in control and in the presence of IQM-266, respectively, $n = 8$,





$p < 0.01$), as well as the inactivation kinetics. In fact, the latter process that exhibits a biexponential decay under control conditions ($\tau_f = 19.6 \pm 2.4$ ms and $\tau_s = 76.2 \pm 9.6$ ms, $n = 14$) becomes monoexponential in the presence of IQM-266 ($\tau = 62.3 \pm 4.7$ ms, $n = 14$, $p > 0.05$ vs. τ_s value in control conditions; **Figures 7C-E**). However, IQM-266 did not increase the charge at any concentration tested (**Figure 7B**). In contrast to what occurs in the presence of DREAM, IQM-266 did not modify the recovery kinetics of inactivation (**Figure 7F**). **Figure 7G** shows the two I-V relationships obtained in the absence and in the presence of IQM-266, together with the ratio $I_{IQM-266}/I_{Control}$ (blue triangles) and the activation

curve (dashed line). A block of the maximum peak current produced by IQM-266 increased in the range of activation of $K_V4.3$ channels but remained constant at membrane potentials positive to +10 mV. IQM-266 did not shift the inactivation curve to more negative potentials (**Figure 7H**), and it did not modify the closed-state inactivation (**Figures 7H,I**). All these results indicate that, although this compound also binds to $K_V4.3$ channels, the increase in the charge observed in $K_V4.3$ /DREAM channels and induced by IQM-266 is due to its specific interaction with DREAM. Moreover, this interaction seems to prevent the effect of DREAM on the recovery from inactivation.



Effect of IQM-266 on I_A From DRG Neurons

DRG neurons are known to express DREAM as well as $K_V4.3$ channels, which contribute to I_A (Phuket and Covarrubias, 2009; Tsantoulas and McMahon, 2014; Tian et al., 2018). Hence, we decided to record I_A from rat DRG neurons in order to evaluate the effect of IQM-266 on native potassium channels. By using a voltage protocol designed to isolate I_A , we recorded transient, fast activating and inactivating potassium currents in the voltage-range in which I_A makes a substantial contribution to voltage-dependent potassium currents (-20 mV to $+20 \text{ mV}$) (Figure 8A). Isolated currents were sensitive to 4-aminopyridine 5 mM (data not shown) and displayed inactivation kinetics that required the sum of two exponential terms for an adequate description. Time constant values and relative amplitude of the fast and slow kinetic components at 0 mV were $\tau_f = 5.1 \pm 0.6 \text{ ms}$ (45%) and $\tau_s = 86.1 \pm 7.5 \text{ ms}$ (55%, $n = 13$ cells). As previously reported, time constants exhibited weak voltage-dependence (Figure 8B), and the relative weight of the two components barely changed in the voltage range that we studied (data not shown; Phuket and Covarrubias, 2009).

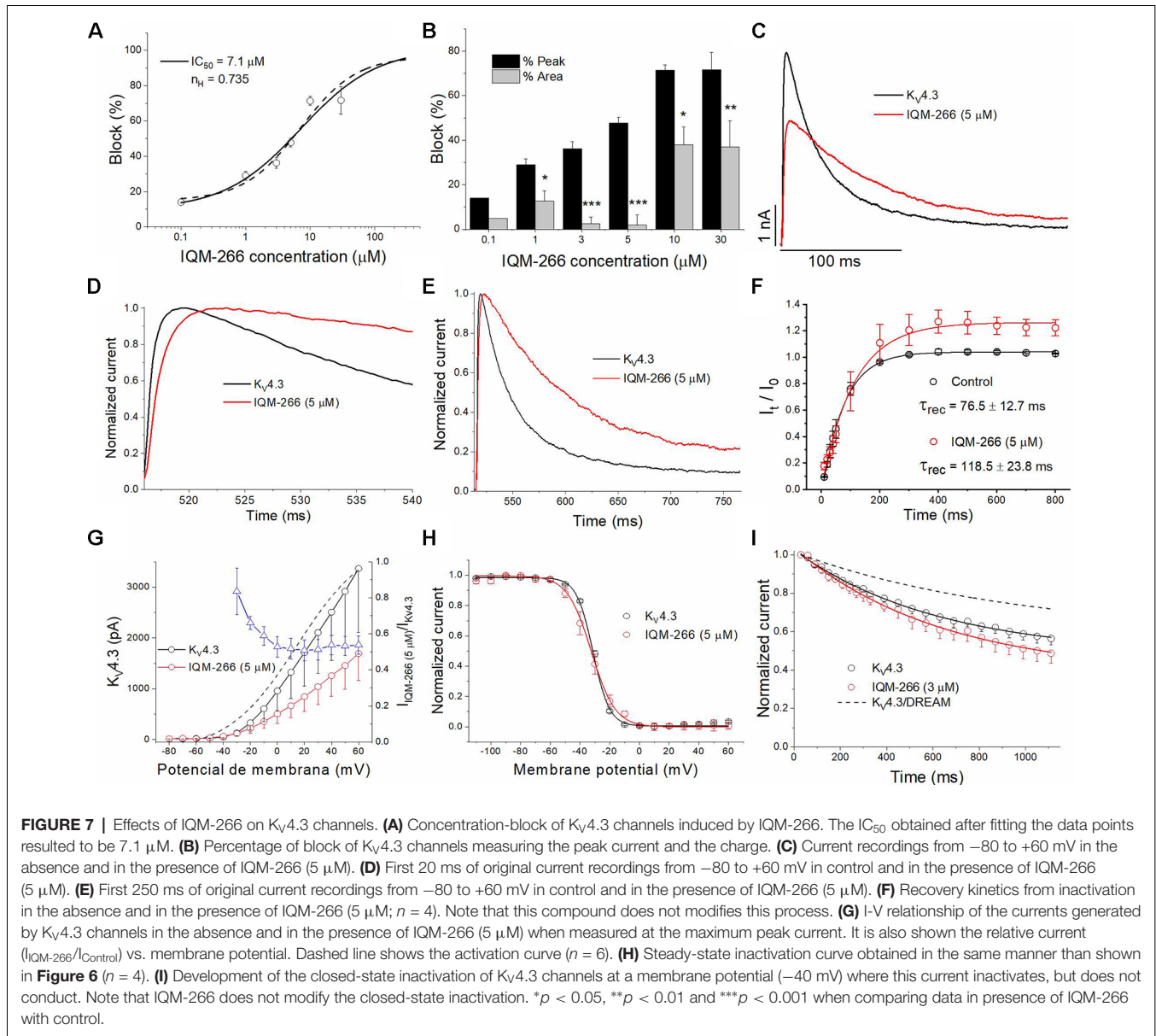
Interestingly, IQM-266 at 3 and $10 \mu\text{M}$ reduced the peak amplitude of I_A dose dependently. Percentage block showed slight voltage dependence, increasing with the depolarization (Figures 8A,B). Likewise, IQM-266 at $10 \mu\text{M}$ slowed current inactivation by increasing both τ_f and τ_s . This effect reached

statistical significance on τ_s and developed in a voltage-dependent manner (at potentials equal and positive to 0 mV ; Figures 8C,D).

DISCUSSION

In the present study the effects of IQM-266 on recombinant $K_V4.3$ and $K_V4.3$ /DREAM channels expressed in mammalian cells, as well as on I_A from DRG neurons, have been analyzed. We demonstrate that this new compound: (1) binds to $K_V4.3$ /DREAM channels in a concentration-, time- and voltage-dependent manner; (2) inhibits the maximum peak current and, to a lesser extent, the charge crossing the cell membrane during depolarization; (3) at certain concentrations ($3 \mu\text{M}$), IQM-266 increases the charge through the cell membrane during the application of depolarizing pulses; and (4) inhibits peak I_A amplitude while slowing its inactivation. Overall, the results presented here are consistent with a preferential binding of IQM-266 to a pre-activated closed state of $K_V4.3$ /DREAM channels.

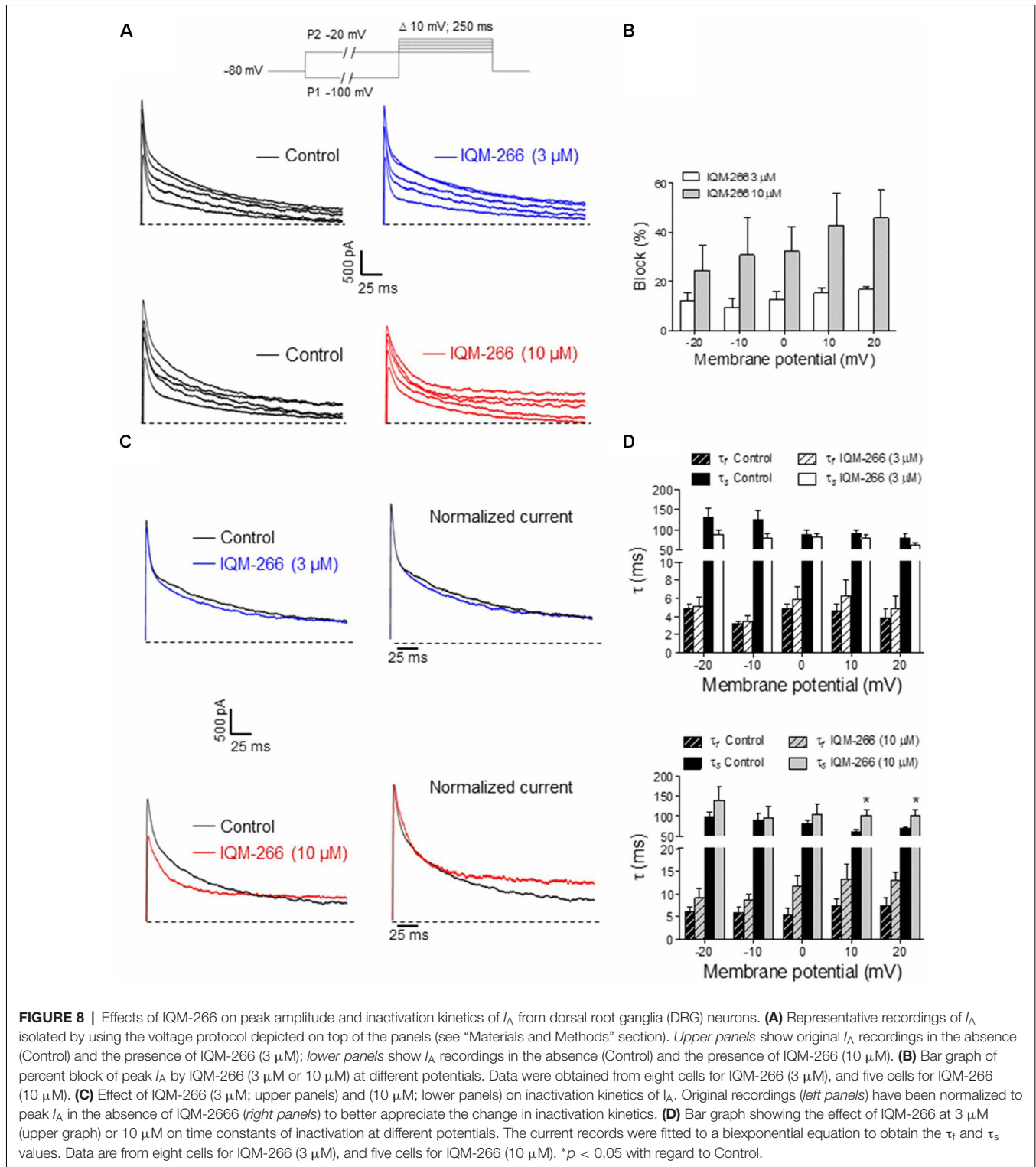
In the last decade, there small molecules have been developed that bind to DREAM and modify K_V4 channel function (Gonzalez et al., 2014; Naranjo et al., 2016). Among them, repaglinide and CL-888 were shown to inhibit I_A , whereas NS5806 would be the only DREAM ligand able to potentiate this



sort of potassium current (Witzel et al., 2012; Gonzalez et al., 2014). Like IQM-266, NS5806 slowed down the inactivation decay of neuronal I_A and slightly decreased the maximum peak current.

The two main reported effects of DREAM on $K_V4.3$ channels are: (i) an increased traffic of $K_V4.3$ channels to the membrane; and (ii) an acceleration of the activation and recovery kinetics from inactivation (An et al., 2000; Naranjo et al., 2016). In the present study, we show that IQM-266 produces the opposite effects to those induced by DREAM: slowing of the activation and recovery from inactivation kinetics, which might be attributed to IQM-266 binding to DREAM, hence supporting the results of the SPR experiments. IQM-266 interacts with $K_V4.3$ /DREAM channels in a concentration-, time- and voltage-dependent manner, consistent with binding preferentially to a pre-activated

closed state of the channels and with very low or no affinity for the open state. There are several pieces of evidence supporting this mechanism of action: (1) the maximum degree of block (produced by $10 \mu\text{M}$ IQM-266, a concentration close to its IC_{50}) measured at the maximum peak and at the charge, was obtained at -10 mV, a potential at which most of the channels are closed or in pre-activated, closed states; (2) block steeply increased in the activation range of $K_V4.3$ /DREAM channels, achieving a maximum and plateau level at potentials positive to $+20$ mV, where the probability of channels opening increases; (3) IQM-266 slows the activation of the $K_V4.3$ /DREAM current. Also, IQM-266 slows the recovery process from inactivation, suggesting that its binding to $K_V4.3$ /DREAM channels promotes inactivation; and (4) in fact, IQM-266 negatively shifted the inactivation curve, as well as the closed-state inactivation.



Since $K_v4.3$ channels mostly inactivate from the closed states (Beck and Covarrubias, 2001), this result is consistent with the interaction of IQM-266 with a closed or pre-activated closed state of the channels (Snyders et al., 1992; Longobardo et al., 1998).

Furthermore, IQM-266 inhibits $K_v4.3$ current in the absence of DREAM. However, the $K_v4.3$ IQM-266 interaction exhibits differential features. In the presence of DREAM, IQM-266 prevents the effect of this regulatory subunit on the channel (acceleration of: (i) recovery from inactivation and activation;

(ii) slower decay kinetics; and (iii) less prominent closed-state inactivation), yet in the absence of DREAM, IQM-266 decreased the peak potassium current and slowed the activation and the inactivation kinetics.

However, the more striking effect produced by IQM-266 is the slowing of inactivation kinetics. Indeed, this effect may explain why at concentrations lower than the IC_{50} , IQM-266 augments the efflux of potassium ions resulting in an increase in charge (activating effect). Importantly, this increase in the charge is observed at membrane potentials positive to +10 mV. This effect is more evident at concentrations at which the inhibition of the maximum peak current is negligible, but still capable of slowing the inactivation decay. This effect could be the basis of a promising therapeutic strategy for the treatment of certain pathologies affecting cardiac (cardiac arrhythmias) or neuronal (epilepsy, Alzheimer disease or ataxia) cells, in which a downregulation of Kv4.3 or DREAM has been demonstrated (Huo et al., 2014; Hall et al., 2015; Smets et al., 2015; Villa and Combi, 2016). IQM-266 also modulated I_A from rat DRG neurons. At 10 μ M, IQM-266 effects on I_A were reminiscent of those observed on heterologously expressed Kv4.3/DREAM channels. Hence, IQM-266 10 μ M inhibited peak I_A , and this effect increased with the depolarization in the physiological range of activation of the current. Likewise, IQM-266 10 μ M slowed inactivation kinetics at potentials positive to 0 mV. In contrast, no facilitation of I_A could be observed with IQM-266 3 μ M. At present, we do not have an explanation for this result except the fact that DRG neurons express other potassium channel regulatory proteins in addition to DREAM (David et al., 2012; Cheng et al., 2016; Tian et al., 2018), which may prevent the potentiating effect seen at 3 μ M IQM-266 on Kv4.3/DREAM channels. Notwithstanding, our results in DRG neurons suggest that IQM-266 constitutes a small, novel chemical molecule suitable to modulate Kv4.3 channels in native systems.

Different neuronal (Hall et al., 2015; Gross et al., 2016) or cardiac pathologies are related to abnormalities in the function of different ion channels and/or regulatory subunits, such as Kv4.3 and the regulatory subunit DREAM. Thus, KChIPs starts

to emerge as a realistic drug target, and IQM-266 could be considered as a new chemical tool that might allow a better understanding of: (i) DREAM physiological role; and (ii) the modulation of I_A in pathological conditions.

AUTHOR CONTRIBUTIONS

DP, PC, LL, PM, YM, PS, CIG, SS and AL-H performed the experiments and analyzed the data. MM-M, LO-O, AA, JN, MG-R and CV conceived the study, analyzed the data and wrote the article.

FUNDING

PC was the recipient of a postgraduate FPI fellowship from the Spanish Ministry of Economy, Industry and Competitiveness (MINECO). This work was funded by the Spanish Ministry of Economy, Industry and Competitiveness (Ministerio de Economía y Competitividad; AEI-FEDER, EU grants): SAF2012-32209 and BFU2015-67284-R (to MG-R), SAF2014-53412-R and SAF2017-89554-R (to JN), SAF2013-45800-R, SAF2016-75021-R (to CV) and SAF2015-66275-C2-2-R (to MM-M); Universidad Complutense de Madrid (UCM) grant: PR75/18-21593 (to AA); the Instituto de Salud Carlos III CIBERNED and CIBERCV programs (to JN and to CV, respectively) and the Madrid regional government/Neurodegenmodels (to JN); Consejo Superior de Investigaciones Científicas (CSIC) grants: PIE 201820E104 (to CV) and 201880E109 (to MG-R and MM-M). We acknowledge support of the publication fee by the CSIC Open Access Publication Support Initiative through its Unit of Information Resources for Research (URICI).

ACKNOWLEDGMENTS

We want to express our thanks to Dr. Snyders for kindly providing us with the cloned pEGFPn1, University of Antwerpen (Belgium) and the Technical Services of the Instituto de Investigaciones Biomedicas Alberto Sols (CSIC-UAM), Madrid, Spain.

REFERENCES

- An, W. F., Bowlby, M. R., Betty, M., Cao, J., Ling, H. P., Mendoza, G., et al. (2000). Modulation of A-type potassium channels by a family of calcium sensors. *Nature* 403, 553–556. doi: 10.1038/35000592
- Bahring, R. (2018). Kv channel-interacting proteins as neuronal and non-neuronal calcium sensors. *Channels* 12, 187–200. doi: 10.1080/19336950.2018.1491243
- Beck, E. J., and Covarrubias, M. (2001). Kv4 channels exhibit modulation of closed-state inactivation in inside-out patches. *Biophys. J.* 81, 867–883. doi: 10.1016/s0006-3495(01)75747-5
- Birnbaum, S. G., Varga, A. W., Yuan, L. L., Anderson, A. E., Sweatt, J. D., and Schrader, L. A. (2004). Structure and function of Kv4-family transient potassium channels. *Physiol. Rev.* 84, 803–833. doi: 10.1152/physrev.00039.2003
- Burgoyne, R. D. (2007). Neuronal calcium sensor proteins: generating diversity in neuronal Ca^{2+} signalling. *Nat. Rev. Neurosci.* 8, 182–193. doi: 10.1038/nrn2093
- Buxbaum, J. D., Choi, E. K., Luo, Y., Lilliehook, C., Crowley, A. C., Merriam, D. E., et al. (1998). Calsenilin: a calcium-binding protein that interacts with the presenilins and regulates the levels of a presenilin fragment. *Nat. Med.* 4, 1177–1181. doi: 10.1038/2673
- Campbell, D. L., Rasmusson, R. L., Qu, Y., and Strauss, H. C. (1993). The calcium-independent transient outward potassium current in isolated ferret right ventricular myocytes. I. Basic characterization and kinetic analysis. *J. Gen. Physiol.* 101, 571–601. doi: 10.1085/jgp.101.4.571
- Carabelli, V., Giannopoli, A., Baldelli, P., Carbone, E., and Artalejo, A. R. (2003). Distinct potentiation of L-type currents and secretion by cAMP in rat chromaffin cells. *Biophys. J.* 85, 1326–1337. doi: 10.1016/S0006-3495(03)74567-6
- Carrion, A. M., Link, W. A., Ledo, F., Mellstrom, B., and Naranjo, J. R. (1999). DREAM is a Ca^{2+} -regulated transcriptional repressor. *Nature* 398, 80–84. doi: 10.1038/18044
- Cheng, H. Y., Pitcher, G. M., Laviolette, S. R., Whishaw, I. Q., Tong, K. I., Kockeritz, L. K., et al. (2002). DREAM is a critical transcriptional repressor for pain modulation. *Cell* 108, 31–43. doi: 10.1016/s0092-8674(01)00629-8
- Cheng, C. F., Wang, W. C., Huang, C. Y., Du, P. H., Yang, J. H., and Tsaur, M. L. (2016). Coexpression of auxiliary subunits KChIP and DPPL in potassium

- channel Kv4-positive nociceptors and pain-modulating spinal interneurons. *J. Comp. Neurol.* 524, 846–873. doi: 10.1002/cne.23876
- David, M., Macias, A., Moreno, C., Prieto, A., Martínez-Mármol, R., Vicente, R., et al. (2012). PKC activity regulates functional effects of Kv α 1.3 on Kv1.5 channels. Identification of a cardiac Kv1.5 channelosome. *J. Biol. Chem.* 287, 21416–21428. doi: 10.1074/jbc.M111.328278
- Franqueza, L., Valenzuela, C., Eck, J., Tamkun, M. M., Tamargo, J., and Snyders, D. J. (1999). Functional expression of an inactivating potassium channel (Kv4.3) in a mammalian cell line. *Cardiovasc. Res.* 41, 212–219. doi: 10.1016/s0008-6363(98)00220-x
- Gonzalez, W. G., Pham, K., and Miksovska, J. (2014). Modulation of the voltage-gated potassium channel (Kv4.3) and the auxiliary protein (KChIP3) interactions by the current activator NS5806. *J. Biol. Chem.* 289, 32201–32213. doi: 10.1074/jbc.M114.577528
- Gross, C., Yao, X., Engel, T., Tiwari, D., Xing, L., Rowley, S., et al. (2016). MicroRNA-mediated downregulation of the potassium channel Kv4.2 contributes to seizure onset. *Cell Rep.* 17, 37–45. doi: 10.1016/j.celrep.2016.08.074
- Hall, A. M., Throesch, B. T., Buckingham, S. C., Markwardt, S. J., Peng, Y., Wang, Q., et al. (2015). Tau-dependent Kv4.2 depletion and dendritic hyperexcitability in a mouse model of Alzheimer's disease. *J. Neurosci.* 35, 6221–6230. doi: 10.1523/JNEUROSCI.2552-14.2015
- Huang, H. Y., Cheng, J. K., Shih, Y. H., Chen, P. H., Wang, C. L., and Tsauro, M. L. (2005). Expression of A-type K⁺ channel α subunits Kv4.2 and Kv4.3 in rat spinal lamina II excitatory interneurons and colocalization with pain-modulating molecules. *Eur. J. Neurosci.* 22, 1149–1157. doi: 10.1111/j.1460-9568.2005.04283.x
- Huo, R., Sheng, Y., Guo, W. T., and Dong, D. L. (2014). The potential role of Kv4.3 K⁺ channel in heart hypertrophy. *Channels* 8, 203–209. doi: 10.4161/chan.28972
- Johnston, J., Forsythe, I. D., and Kopp-Scheinflug, C. (2010). Going native: voltage-gated potassium channels controlling neuronal excitability. *J. Physiol.* 588, 3187–3200. doi: 10.1113/jphysiol.2010.191973
- Johnsson, B., Löfås, S., and Lindquist, G. (1991). Immobilization of proteins to a carboxymethyl-dextran-modified gold surface for biospecific interaction analysis in surface plasmon resonance sensors. *Anal. Biochem.* 198, 268–277. doi: 10.1016/0003-2697(91)90424-r
- Lilliehook, C., Chan, S., Choi, E. K., Zaidi, N. F., Wasco, W., Mattson, M. P., et al. (2002). Calsenilin enhances apoptosis by altering endoplasmic reticulum calcium signaling. *Mol. Cell. Neurosci.* 19, 552–559. doi: 10.1006/mcne.2001.1096
- Longobardo, M., Delpon, E., Caballero, R., Tamargo, J., and Valenzuela, C. (1998). Structural determinants of potency and stereoselective block of hKv1.5 channels induced by local anesthetics. *Mol. Pharmacol.* 54, 162–169. doi: 10.1124/mol.54.1.162
- López-Hurtado, A., Burgos, D. F., González, P., Dopazo, X. M., González, V., Rábano, A., et al. (2018). Inhibition of DREAM-ATF6 interaction delays onset of cognition deficit in a mouse model of Huntington's disease. *Mol. Brain* 11:13. doi: 10.1186/s13041-018-0359-6
- Maffie, J., and Rudy, B. (2008). Weighing the evidence for a ternary protein complex mediating A-type K⁺ currents in neurons. *J. Physiol.* 586, 5609–5623. doi: 10.1113/jphysiol.2008.161620
- Moreno, C., Oliveras, A., Bartolucci, C., Munoz, C., de la Cruz, A., Peraza, D. A., et al. (2017). D242N, a Kv7.1 LQTS mutation uncovers a key residue for IKs voltage dependence. *J. Mol. Cell. Cardiol.* 110, 61–69. doi: 10.1016/j.yjmcc.2017.07.009
- Nadal, M. S., Ozaita, A., Amarillo, Y., Vega-Saenz de Miera, E., Ma, Y., Mo, W., et al. (2003). The CD26-related dipeptidyl aminopeptidase-like protein DPPX is a critical component of neuronal A-type K⁺ channels. *Neuron* 37, 449–461. doi: 10.1016/s0896-6273(02)01185-6
- Naranjo, J. R., Zhang, H., Villar, D., González, P., Dopazo, X. M., Morón-Oset, J., et al. (2016). Activating transcription factor 6 derepression mediates neuroprotection in Huntington disease. *J. Clin. Invest.* 126, 627–638. doi: 10.1172/jci82670
- Phuket, T. R., and Covarrubias, M. (2009). Kv4 channels underlie the subthreshold-operating A-type K⁺-current in nociceptive dorsal root ganglion neurons. *Front. Mol. Neurosci.* 2:3. doi: 10.3389/neuro.02.003.2009
- Radicke, S., Vaquero, M., Caballero, R., Gómez, R., Núñez, L., Tamargo, J., et al. (2008). Effects of MiRP1 and DPP6 β -subunits on the blockade induced by flecainide of Kv4.3/KChIP2 channels. *Br. J. Pharmacol.* 154, 774–786. doi: 10.1038/bjp.2008.134
- Ruiz-Gomez, A., Mellström, B., Tornero, D., Morato, E., Savignac, M., Holguín, H., et al. (2007). G protein-coupled receptor kinase 2-mediated phosphorylation of downstream regulatory element antagonist modulator regulates membrane trafficking of Kv4.2 potassium channel. *J. Biol. Chem.* 282, 1205–1215. doi: 10.1074/jbc.M607166200
- Seródi, P., and Rudy, B. (1998). Differential expression of Kv4 K⁺ channel subunits mediating subthreshold transient K⁺ (A-type) currents in rat brain. *J. Neurophysiol.* 79, 1081–1091. doi: 10.1152/jn.1998.79.2.1081
- Smets, K., Duarri, A., Deconinck, T., Ceulemans, B., van de Warrenburg, B. P., Zuchner, S., et al. (2015). First *de novo* KCND3 mutation causes severe Kv4.3 channel dysfunction leading to early onset cerebellar ataxia, intellectual disability, oral apraxia and epilepsy. *BMC Med. Genet.* 16:51. doi: 10.1186/s12881-015-0200-3
- Snyders, D. J., Knoth, K. M., Roberds, S. L., and Tamkun, M. M. (1992). Time-, voltage-, and state-dependent block by quinidine of a cloned human cardiac potassium channel. *Mol. Pharmacol.* 41, 322–330.
- Tian, N. X., Xu, Y., Yang, J. Y., Li, L., Sun, X. H., Wang, Y., et al. (2018). KChIP3 N-terminal 31–50 fragment mediates its association with TRPV1 and alleviates inflammatory hyperalgesia in rats. *J. Neurosci.* 38, 1756–1773. doi: 10.1523/JNEUROSCI.2242-17.2018
- Tsantoulas, C., and McMahon, S. B. (2014). Opening paths to novel analgesics: the role of potassium channels in chronic pain. *Trends Neurosci.* 37, 146–158. doi: 10.1016/j.tins.2013.12.002
- Valenzuela, C., Sánchez Chapula, J., Delpón, E., Elizalde, A., Pérez, O., and Tamargo, J. (1994). Imipramine blocks rapidly activating and delays slowly activating K⁺ current activation in guinea pig ventricular myocytes. *Circ. Res.* 74, 687–699. doi: 10.1161/01.res.74.4.687
- Villa, C., and Combi, R. (2016). Potassium channels and human epileptic phenotypes: an updated overview. *Front. Cell. Neurosci.* 10:81. doi: 10.3389/fncel.2016.00081
- Wettwer, E., Amos, G., Gath, J., Zerkowski, H. R., Reidemeister, J. G., and Ravens, U. (1993). Transient outward current in human and rat ventricular myocytes. *Cardiovasc. Res.* 27, 1662–1669. doi: 10.1093/cvr/27.9.1662
- Witzel, K., Fischer, P., and Bähring, R. (2012). Hippocampal A-type current and Kv4.2 channel modulation by the sulfonylurea compound NS5806. *Neuropharmacology* 63, 1389–1403. doi: 10.1016/j.neuropharm.2012.08.017
- Wu, L. J., Mellström, B., Wang, H., Ren, M., Domingo, S., Kim, S. S., et al. (2010). DREAM (downstream regulatory element antagonist modulator) contributes to synaptic depression and contextual fear memory. *Mol. Brain* 3:3. doi: 10.1186/1756-6606-3-3
- Zhang, M., Jiang, M., and Tseng, G. N. (2001). minK-related peptide 1 associates with Kv4.2 and modulates its gating function: potential role as β subunit of cardiac transient outward channel? *Circ. Res.* 88, 1012–1019. doi: 10.1161/hh1001.090839

Conflict of Interest Statement: The authors declare that the research was conducted in the absence of any commercial or financial relationships that could be construed as a potential conflict of interest.

Copyright © 2019 Peraza, Cercos, Miaja, Merinero, Lagartera, Socuëllamos, Izquierdo García, Sánchez, López-Hurtado, Martín-Martínez, Olivares-Oré, Naranjo, Artalejo, Gutiérrez-Rodríguez and Valenzuela. This is an open-access article distributed under the terms of the Creative Commons Attribution License (CC BY). The use, distribution or reproduction in other forums is permitted, provided the original author(s) and the copyright owner(s) are credited and that the original publication in this journal is cited, in accordance with accepted academic practice. No use, distribution or reproduction is permitted which does not comply with these terms.